Plastic Flow of the Mechanically Alloyed Fe–0.6%O at Temperatures of 550–700°C

V. A. Dudko[a], R. O. Kaibyshev[a], A. N. Belyakov[a], Y. Sakai[b], and K. Tsuzaki[b]

[a] *Belgorod State University, ul. Pobedy 85, Belgorod, 308015 Russia*

[b] *National Institute for Materials Science, 1-2-1 Sengen, Tsukuba, Ibaraki, 3050047 Japan*

Abstract—Creep of steel Fe–0.6%O produced by the method of powder metallurgy has been studied in a temperature range of 550–700°C at flow stresses from 100 to 400 MPa. It has been shown that the creep of the material is characterized by high values of the apparent activation energy for deformation, which considerably exceeds the value of the activation energy for self-diffusion in α iron, and by high values of the stress exponent in the power law of creep. An analysis of the deformation behavior of the alloy showed that there are observed high threshold stresses as a result of retardation of moving dislocations by small incoherent particles of oxides. Taking into account the threshold stresses and the temperature dependence of the shear modulus, it has been established that the deformation behavior of the powder material is described by a power law of creep. The true values of the stress exponent were found to be approximately 8, and the values of the true activation energy for deformation, to be close to the activation energy for bulk (at T = 700°C) and pipe (at T = 550–650°C) self-diffusion.

1. INTRODUCTION

At present, to increase the creep strength of superalloys, various indissoluble dispersed particles are introduced into the metallic matrix of the alloys by different methods of powder metallurgy. One of such methods is the mechanical milling of powders of various materials and their subsequent compacting by plastic treatment [1, 2]. This method is very efficient, since it makes it possible to obtain articles of commercial sizes made from an unlimited number of materials. This method was recently used for obtaining high-strength steels with an ultrafine-grain structure containing nanoparticles of oxides that are homogeneously distributed in the ferrite matrix [3, 4].

The strain rate $\dot{\varepsilon}$ at the steady-state stage of plastic flow of materials that do not contain dispersed particles is usually described at elevated temperatures by a power dependence on the applied stress [5–7]

$$\dot{\varepsilon} = A\sigma^n \exp\left(\frac{-Q}{RT}\right), \quad (1)$$

where A is a constant, σ is the applied flow stress, n is the stress exponent, Q is the activation energy for plastic deformation, R is the universal gas constant, and T is the absolute temperature. In different materials the stress exponent varies from 3 to 7, depending on the mechanisms of motion and interaction of dislocations. The value n = 3 is observed in the case of a viscous glide of dislocation, i.e., if the rate of dislocation movement is determined by the velocity of migration of the Cottrell atmosphere of solute atoms existing around the dislocation core [6]. In pure metals and solid solutions the stress exponent is equal to 4–7. In this case the plastic-flow velocity is controlled by the velocity of a nonconservative movement of dislocations, namely, by their climb [6]. An increase in the magnitude of the stress exponent was observed in the case of high rates of deformation [5–7]. Usually this is ascribed to a disturbance of the power law of creep. In the overwhelming majority of cases the experimental values of the activation energy for deformation coincide with the activation energy for bulk, pipe, or grain-boundary self-diffusion. However, in the range of comparatively low temperatures of deformation the mechanisms of plastic flow have been studied insufficiently. This especially refers to oxide-dispersion-strengthened (ODS) alloys, whose deformation behavior was mainly investigated at high homologous temperatures [8–14]. Furthermore, the works published were as a rule performed on materials in which the basic (matrix) phase was a solid solution with a face-centered cubic lattice. Any systematic studies of the mechanisms of deformation in the ODS alloys with a body-centered cubic structure are virtually absent.

This work is aimed at an experimental study of the mechanisms of plastic flow in an Fe–O alloy (containing about 2 vol % iron oxide Fe_3O_4 with an average particle size of ~11 nm [4]) at temperatures of 550–700°C, an analysis of the dependence of the velocity of plastic

flow on the applied stress, and the determination of the magnitude of threshold stresses and of the effect of the temperature of treatment on it.

2. EXPERIMENTAL

As the material for the study, we selected steel Fe–0.6%O, which contains (in wt %) 0.58 O, 1.2 Cr, 0.5 Ni, 0.18 Mn, 0.11 W, 0.11 Si, 0.05 Cu, 0.01 C, 0.009 P, 0.007 S, and Fe for balance. The oxygen in this steel is mainly concentrated in small dispersed particles (~11 nm) of the iron oxide Fe_3O_4, whose volume fraction is approximately 2% [4]. The method of the steel preparation, which consists of mechanical milling and subsequent consolidation by plastic deformation, was in detail described earlier [3, 4, 15]. To stabilize the structure, the bars were annealed at 810°C for 25 h prior to the mechanical tests.

The mechanical tests were carried out in a temperature range of 550–700°C. At high strain rates (from 1.4×10^{-6} to 10^{-2} s^{-1}), the method of compressive loading was employed, with the use of a Schenk RMS100 universal testing machine. At low strain rates (from 1.2×10^{-8} to 10^{-5} s^{-1}), the method of tensile tests under a constant load was employed, with the use of a creep testing machine of a lever type. The compression samples had a diameter of 7 mm and a height of 11 mm; the tensile samples had the length of the gage part equal to 20 mm with a diameter of 4 mm. The axis of each sample coincided with the direction of the preceding plastic treatment. For the protection from oxidation the samples were covered with a lubricant, which consisted of the oxides of boron and aluminum. In more detail, the methods of mechanical testing are described in [16, 17].

The microstructure was studied in a JEM-2000E transmission electron microscope (TEM). The foils for TEM studies were prepared using a Tenupol-3 electropolishing device with a 5% solution of perchloric acid in the acetic acid under a voltage of 60 V at room temperature.

3. RESULTS

3.1. Mechanical Properties

Figure 1 displays typical dependences of creep rate on strain at temperatures of 600 and 700°C at different stresses. It is seen that all creep curves have a short first transient stage of creep. At the early stage of plastic flow, the strain rate decreases sharply to a certain minimum value, which is kept constant during further deformation. The plastic flow reaches a steady-state stage. The minimum creep rate is reached at comparatively small strains $\varepsilon < 0.012$.

Dependence of the minimum creep rate on the applied stress. Assuming that the deformation behavior of the material is described by a power law of creep (1), let us examine the dependence of the strain rate on the flow stress. Figure 2 displays, in the logarithmic coordinates, a change in the strain rate with a change in the applied stress at different test temperatures. It is seen that the stress exponent calculated from the experiment has anomalously high values (~16). Furthermore,

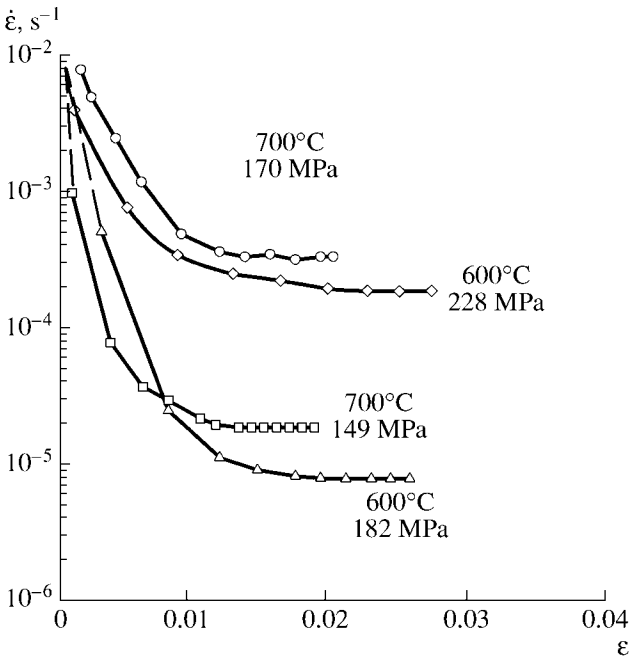

Fig. 1. Dependence of the true creep rate on strain for the Fe–0.6%O alloy.

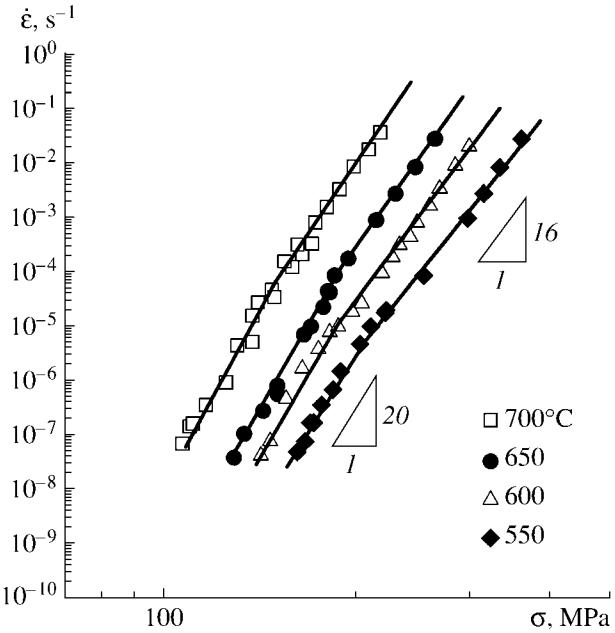

Fig. 2. Relationship between the creep rate and the applied stress at different temperatures in the logarithmic coordinates.

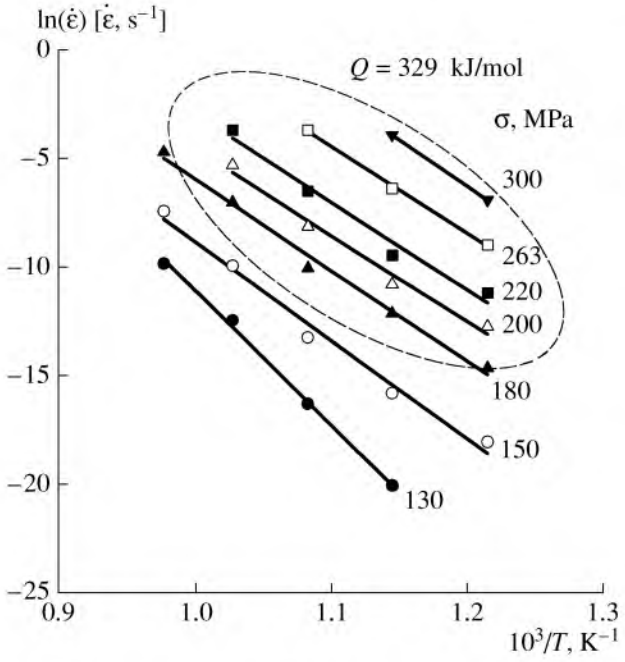

Fig. 3. Creep rate at different applied stresses as a function of the reciprocal absolute temperature.

Fig. 4. Interaction of dislocations with dispersed particles in the Fe–0.6%O alloy after creep at 600°C at a strain rate $\dot{\varepsilon} = 1.3 \times 10^{-7}$ s^{-1}.

the stress exponent increases with decreasing creep rate. The results obtained do not agree with the traditional deformation behavior of metallic materials at elevated temperatures and indicate the presence of threshold stresses [19–21, 23].

Temperature dependence of the minimum creep rate. For determining the temperature dependence of the minimum creep rate, we used a mathematical analysis of Eq. (1). Plots of the logarithm of the minimum creep rate on the reciprocal absolute temperature were constructed at different constant applied stresses (Fig. 3). In the range of high experimental strain rates, the straight lines ($\ln(\dot{\varepsilon}) = f(1/T)$) corresponding to different applied stresses have the same slope, which makes it possible to estimate the apparent activation energy Q by measuring the slope Q/R (Fig. 3). The experimental activation energy for deformation was found to be 329 kJ/mol. This value considerably exceeds the activation energy for bulk self-diffusion in α iron (Q_1 = 251 kJ/mol [6]), which also can indicate the existence of threshold stresses.

3.2. Microstructural Studies

It has been shown in [15] that the annealing of the steel under consideration at temperatures below 900°C does not lead to considerable grain growth; the average grain size after annealing is ~0.5 μm. It was also shown by TEM that the particles of the iron oxide have a spherical equiaxed shape with a diameter in the range from 5 to 50 nm. The particles are uniformly distributed in the ferrite matrix. The average distance between the particles is approximately 200 nm. In all deformed samples, there was revealed an interaction between the dislocations and the dispersed particles (Fig. 4). The particles play the role of efficient obstacles for the movement of dislocations. The strongly curved configurations of lattice dislocations shown in Fig. 4 can be explained on the basis of the model of local climb of dislocations [13, 14] or of the model of the detachment of dislocations from the particles [18]. No noticeable temperature effect on the dislocation structure was found. The creep rate also does not have a noticeable effect on the microstructure parameters.

4. DISCUSSION

The deformation behavior of steel Fe–0.6%O is characterized by high experimental values of the activation energy for deformation and also by a decrease in the coefficient of strain-rate sensitivity with decreasing flow stresses. Analogous results were reported in some works devoted to studies of dispersion-strengthened alloys [10–12, 19–21]. The dispersion-strengthened materials are usually characterized by the increased resistance to creep up to high homologous temperatures as a result of the presence in them of the so-called threshold stresses σ_{th} below which the rate of plastic flow is negligibly small. When analyzing the deformation behavior of such alloys, there is introduced a concept of effective flow stresses $\sigma_{eff} = \sigma - \sigma_{th}$, which are obtained by subtracting the threshold stress from the applied stress [19]. In this case, the deformation behavior of material is described by the following equation:

$$\dot{\varepsilon} = A\left(\frac{\sigma - \sigma_{th}}{G}\right)^n \exp\left(\frac{-Q_c}{RT}\right), \qquad (2)$$

where G is the shear modulus, and n and Q_c are the true stress exponent and the true activation energy for defor-

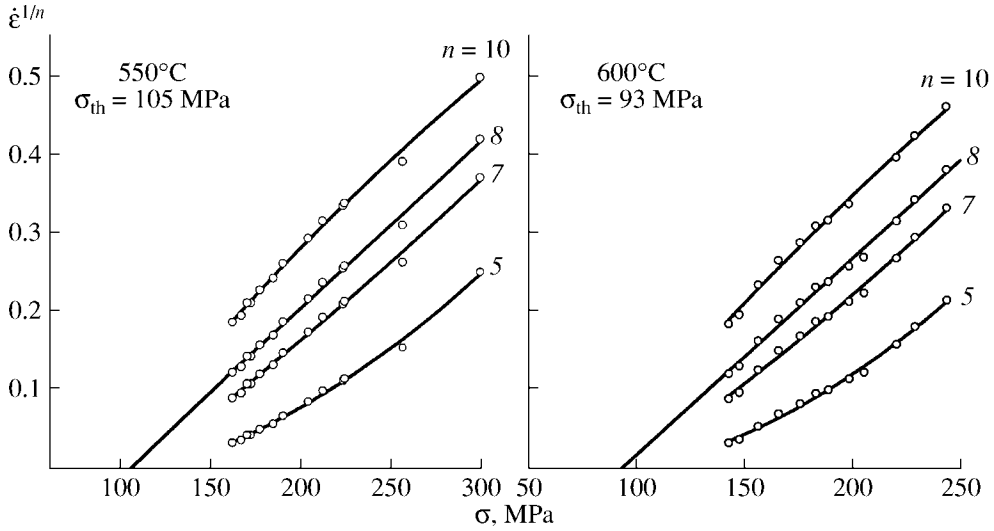

Fig. 5. Typical relationships between $\dot{\varepsilon}^{1/n}$ and σ for the determination of threshold stresses at different n.

mation, respectively. In practice, the threshold stresses, as a rule, are equal to the long-term strength, which makes it possible to use the ODS alloys as high-temperature materials (superalloys) for the operation under loads that considerably exceed those for the materials that do not contain nanooxides.

Determining threshold stresses. To estimate threshold stresses, we plotted dependences of $\dot{\varepsilon}^{1/n}$ on σ for each deformation temperature. The typical dependences for different $\dot{\varepsilon}^{1/n}$ are shown in Fig. 5. As the true value of n^*, we chose the value of n for which the experimental points fall well into a straight line. It was established that the $\dot{\varepsilon}^{1/n}$ (σ) graphs are approximated by a linear dependence with a maximum regression coefficient at n = 8. The threshold stresses are determined by the extrapolation of the resultant straight lines to $\dot{\varepsilon}^{1/n} = 0$; the corresponding value of σ is taken as the threshold stress. The experimental values of the threshold stresses are given in Table 1. The absolute values of the threshold stresses in the material investigated are sufficiently high; in many instances, they are greater than half the applied stress. It is seen that the ODS iron can carry quite high loads, as the most contemporary high-temperature steels with a dislocation martensite structure [22]. Thus, the strengthening of steels by nanooxides can be considered as a highly efficient method of increasing creep strength. Note also that the deformation temperature has only a weak effect on the value of threshold stresses. The observed temperature dependence of threshold stresses is very weak and can be connected only with the temperature dependence of the shear modulus; i.e., in this case (in contrast to the results obtained in [16, 17, 19–21, 23, 24]) no temperature dependence of the threshold stresses normalized to the shear modulus has been revealed. Correspondingly, the threshold behavior can be analyzed in terms of the existing models, most of which do not predict a temperature dependence of threshold stresses [25].

Origin of threshold stresses. It is usually assumed that the sources of threshold stresses are stable incoherent dispersed particles, which serve as efficient barriers for mobile dislocations. In the Fe–0.6%O alloy we investigate here, the factor responsible for the existence of threshold stresses can be the presence of dispersed particles of the iron oxide. Let us consider the mechanism of interaction of moving dislocations with particles. There exist several theoretical models of the mechanism of strengthening of alloys by dispersed particles, e.g., the Orowan model [23], the model of the local climb of dislocations through particles [24], the model of the dislocation detachment from the particle [18]. The values of threshold stresses calculated in different models are given in Table 2. The following structural parameters were used for the calculations: the diameter of particles, d = 10 mm; the interparticle distance, λ = 200 nm; the Burgers vector of dislocations, b = 0.248 nm for α-Fe; and the parameter of relaxation, k_d = 0.9. The experimental values of threshold stresses coincide sufficiently well with those calculated in the models of local climb of dislocations and of the detachment of dislocations from particles (see Table 1). The structural studies (see Fig. 4) also indicate that the over-

Table 1. Experimental values of threshold stresses in the Fe–0.6%O alloy at different deformation temperatures

T, °C	550	600	650	700
σ_{th}, MPa	100	95	90	80
σ_{th}/G	1.6×10^{-3}	1.58×10^{-3}	1.58×10^{-3}	1.5×10^{-3}

Table 2. Threshold stresses (MPa) of the Fe–0.6%O alloy calculated using different theoretical models for the incoherent dispersed particles

Model	Magnitude of σ_{th}	550°C	600°C	650°C	700°C
Orowan [23]	$\sigma_o = 0.84Eb/(\lambda - d)$	377.3	361.1	342.6	321.7
Local climb [24]	$\sigma_b = 0.3Eb/\lambda$	121.3	116.1	110.1	103.4
Breakaway [18]	$\sigma_d = Eb/\lambda(1 - k_d^2)^{1/2}$	127.8	122.3	116.1	109

coming of particles by moving dislocations occurs by bypassing of particles by the dislocations without the formation of characteristic Orowan loops. This bypassing is characteristic of the bypassing of particles by dislocations by the mechanism of local climb. As was shown in [24], the dislocation line which contains a half-loop sufficient for overcoming a nanoparticle can be stable only in the case of its interaction with the interphase boundary. This interaction decreases the dislocation energy due to a partial relaxation of its long-range stress fields near the interphase boundary and is the factor responsible for the appearance of threshold stresses necessary for the breakaway of a dislocation from the particle. Consequently, the strengthening effect of dispersed oxides in the Fe–0.6%O alloy is ensured due to an increase in the overall length of dislocations during their interaction with the particles and to an increase in the energy necessary for the breakaway of dislocations from the particles.

Deformation behavior with allowance for threshold stresses. To analyze the deformation behavior of the Fe–0.6%O alloy, the data of mechanical tests were revised with allowance for threshold stresses according to Eq. (2). The dependences of the creep rate on the effective flow stresses normalized to the shear modulus are presented in Fig. 6. The deformation behavior of the alloy at temperatures of 550–700°C is described well by a power law of creep in the form (2) with a true stress exponent $n = 8$ in a wide range of strain rates from 10^{-8} to 10^{-1} s^{-1}.

The true activation energy for plastic deformation Q_c in Eq. (2) was determined by the method described above, with the use of values of effective stresses. The thus-calculated values of Q_c are given in Fig. 7 as a function of the deformation temperature. It is seen that the magnitude of the true activation energy equal to 185 ± 15 kJ/mol at temperatures in the range from 550 to 650°C is very close to the value for pipe self-diffusion in pure α iron (Q_p = 174 kJ/mol [6]). At a higher testing temperature (700°C), the activation energy for deformation increases to 259 ± 15 kJ/mol, which coincides with the activation energy for bulk self-diffusion.

Thus, as a result of the analysis of the deformation behavior of the Fe–0.6%O alloy with allowance for

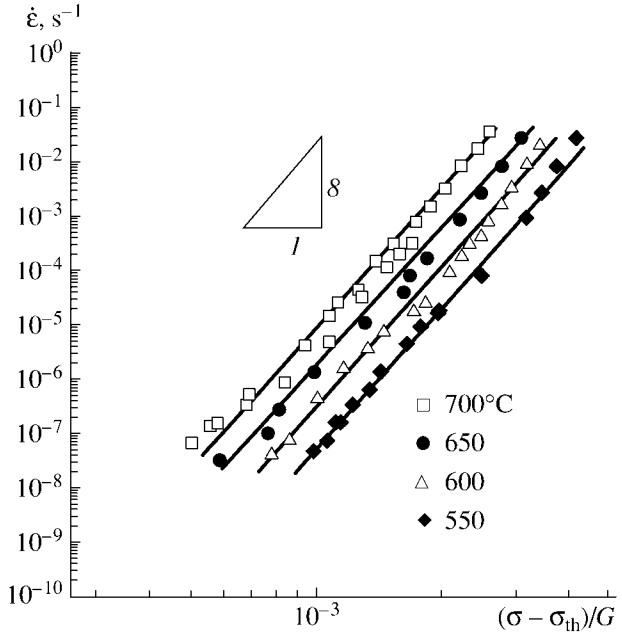

Fig. 6. Variation of the logarithm of the creep rate depending on the logarithm of effective flow stress normalized to the shear modulus.

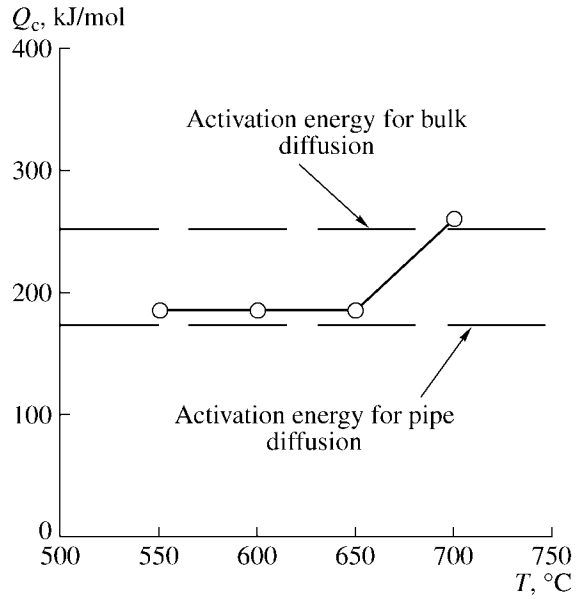

Fig. 7. Temperature dependence of the activation energy for creep.

threshold stresses, we obtained realistic values of the true activation energy for deformation. It can be concluded that the creep rate of alloy in the temperature range of 550–650°C is determined by the nonconservative movement of dislocations, which, in turn, is controlled by self-diffusion along dislocation cores. At a deformation temperature of 700°C, the mechanism that controls the climb of dislocations is bulk self-diffusion.

CONCLUSIONS

(1) The deformation behavior of the Fe–0.6%O alloy containing dispersed oxides whose volume fraction is 2% has been investigated in the temperature range of 550–700°C. It is shown that the dispersed particles retard the dislocation movement and thus exert a substantial influence on the deformation behavior of the alloy. The threshold stresses during creep are approximately 100 MPa.

(2) The relationship between the strain rate and the effective flow stress calculated with allowance for threshold stresses can be represented in the form of a power law with a stress exponent equal to 8. The true activation energies for deformation in the temperature range of 550–650°C and at a temperature of 700°C are 185 ± 15 and 259 ± 15 kJ/mol, respectively.

(3) The overcoming of dispersed particles by dislocations in the process of plastic flow at temperatures of 550–650°C is controlled by pipe self-diffusion, and at a temperature of 700°C, by bulk self-diffusion.

REFERENCES

1. Y. Kimura and S. Takaki, "Microstructural Changes during Annealing of Work-Hardened Mechanically Milled Metallic Powders," Mater. Trans. JIM **36**, 289–296 (1995).
2. Y. Kimura, S. Takaki, S. Suejima, et al., "Ultra Grain Refining and Decomposition of Oxide during Super-Heavy Deformation in Oxide Dispersion Ferritic Stainless Steel Powder," ISIJ Int. **39**, 176–182 (1999).
3. A. Belyakov, Y. Sakai, T. Hara, et al., "Effect of Dispersed Particles on Microstructure Evolved in Iron under Mechanical Milling Followed by Consolidating Rolling," Metall. Mater. Trans. A **32A**, 1769–1776 (2001).
4. A. Belyakov, Y. Sakai, T. Hara, et al., "Evolution of Submicrocrystalline Iron Containing Dispersed Oxides under Mechanical Milling Followed by Consolidation," Metall. Mater. Trans. A **33A**, 3241–3248 (2002).
5. J. Čadek, *Creep in Metallic Materials* (Academia, Prague, 1994).
6. H. J. Frost and M. F. Ashby, *Deformation-Mechanisms Maps* (Pergamon, Oxford, 1982; Metallurgiya, Chelyabinsk, 1989).
7. S. V. Raj and T. G. Langdon, "Creep Behavior of Copper at Intermediate Temperatures—I. Mechanical Characteristics," Acta Metall. **37**, 843–852 (1989).
8. S. E. Broyles, K. R. Anderson, J. R. Groza, and J. C. Gibeling, "Creep Deformation of Dispersion-Strengthened Copper," Metall. Mater. Trans. A **27** (5), 1217–1227 (1996).
9. D. C. Dunand and A. M. Jansen, "Creep of Metals Containing High Volume Fractions of Unshearable Dispersoids—Part I. Modeling the Effect of Dislocation Pile-Ups upon the Detachment Threshold Stress," Acta Mater. **45** (11), 4569–4581 (1997).
10. J. Čadek, S. J. Zhu, and K. Milička, "Threshold Creep Behavior of Aluminium Dispersion Strengthened by Fine Alumina Particles," Mater. Sci. Eng., A **252** (1), 1–5 (1998).
11. J. Čadek, K. Kucharova, and S. J. Zhu, "Creep Behaviour of an Oxide Dispersion Strengthened Al–5Mg Alloy Reinforced by Silicon Carbide Particulates—An Oxide Dispersion Strengthened Al–5Mg–30SiC_p Composite," Mater. Sci. Eng., A **272** (1), 45–56 (1999).
12. J. Čadek, K. Kucharova, and S. J. Zhu, "Disappearance of the True Threshold Creep Behavior of an ODS Al–30SiC_p Composite at High Temperatures," Mater. Sci. Eng., A **281** (1–2), 162–168 (2000).
13. D. Haussler, M. Bartsch, U. Messerschmidt, and B. Reppich, "HVTEM in Situ Observations of Dislocation Motion in the Oxide Dispersion Strengthened Superalloy MA 754," Acta Mater. **49** (18), 3647–3657 (2001).
14. A. Wasilkowska, M. Bartsch, and U. Messerschmidt, "Creep Mechanisms of Ferritic Oxide Dispersion Strengthened Alloys," J. Mater. Proc. Techn. **133** (1–2), 218–224 (2003).
15. A. Belyakov, Y. Sakai, T. Hara, et al., "Effect of Nano-Sized Oxides on Annealing Behaviour of Ultrafine Grained Steels," Mater. Trans. **45** (7), 1–7 (2004).
16. R. Kaibyshev and I. Kazakulov, "Deformation Behavior of Fe–3Si Steel," Mater. Sci. Technol. **20** (2), 221–228 (2004).
17. R. Kaibyshev, O. Sitdikov, I. Mazurina, and D. R. Lesuer, "Deformation Behavior of a 2219 Al Alloy," Mater. Sci. Eng., A **334** (1–2), 104–113 (2002).
18. J. Rösler and E. Arzt, "A New Model-Based Creep Equation for Dispersion Strengthened Materials," Acta Metall. Mater. **38**, 671–683 (1990).
19. K. T. Park, E. Lavernia, and F. Mohamed, "High-Temperature Deformation of 6061 Al," Acta Metall. Mater. **42** (3), 667–678 (1994).
20. Y. Li, S. R. Nutt, and F. Mohamed, "An Investigation of Creep and Substructure Formation in 2124 Al," Acta Mater. **45** (6), 2607–2620 (1997).
21. A. B. Pandey, R. S. Mishra, A. G. Paradkar, and Y. R. Mahajan, "Steady State Creep Behavior of an Al–Al_2O_3 Alloy," Acta Mater. **45** (3), 1297–1306 (1997).
22. K. Yamada, M. Igarashi, S. Muneki, and F. Abe, "Effect of Co Addition on Microstructure in High Cr Ferritic Steels," ISIJ Int. **43** (9), 1438–1443 (2003).
23. F. A. Mohamed, K. T. Park, and E. J. Lavernia, "Creep Behavior of Discontinuous SiC–Al Composites," Mater. Sci. Eng., A **150** (1), 21–35 (1992).
24. E. Arzt and D. Wilkinson, "Threshold Stresses for Dislocation Climb over Hard Particles: The Effect of an Attractive Interaction," Acta Metall. **34**, 1893–1898 (1986).
25. R. Kaibyshev, F. Musin, E. Avtokratova, and Y. Motohashi, "Deformation Behavior of a Modified 5083 Aluminum Alloy," Mater. Sci. Eng., A **392** (1–2), 373–379 (2005).